

An Improved Limit for Γ_{ee} of $X(3872)$ and Γ_{ee} Measurement of $\psi(3686)$

M. Ablikim¹, M. N. Achasov^{9,a}, X. C. Ai¹, O. Albayrak⁵, M. Albrecht⁴, D. J. Ambrose⁴⁴,
A. Amoroso^{48A,48C}, F. F. An¹, Q. An⁴⁵, J. Z. Bai¹, R. Baldini Ferroli^{20A}, Y. Ban³¹, D. W. Bennett¹⁹,
J. V. Bennett⁵, M. Bertani^{20A}, D. Bettoni^{21A}, J. M. Bian⁴³, F. Bianchi^{48A,48C}, E. Boger^{23,h},
O. Bondarenko²⁵, I. Boyko²³, R. A. Briere⁵, H. Cai⁵⁰, X. Cai¹, O. Cakir^{40A,b}, A. Calcaterra^{20A},
G. F. Cao¹, S. A. Cetin^{40B}, J. F. Chang¹, G. Chelkov^{23,c}, G. Chen¹, H. S. Chen¹, H. Y. Chen²,
J. C. Chen¹, M. L. Chen¹, S. J. Chen²⁹, X. Chen¹, X. R. Chen²⁶, Y. B. Chen¹, H. P. Cheng¹⁷,
X. K. Chu³¹, G. Cibinetto^{21A}, D. Cronin-Hennessy⁴³, H. L. Dai¹, J. P. Dai³⁴, A. Dbeyssi¹⁴, D. Dedovich²³,
Z. Y. Deng¹, A. Denig²², I. Denysenko²³, M. Destefanis^{48A,48C}, F. De Mori^{48A,48C}, Y. Ding²⁷, C. Dong³⁰,
J. Dong¹, L. Y. Dong¹, M. Y. Dong¹, S. X. Du⁵², P. F. Duan¹, J. Z. Fan³⁹, J. Fang¹, S. S. Fang¹,
X. Fang⁴⁵, Y. Fang¹, L. Fava^{48B,48C}, F. Feldbauer²², G. Felici^{20A}, C. Q. Feng⁴⁵, E. Fioravanti^{21A}, M.
Fritsch^{14,22}, C. D. Fu¹, Q. Gao¹, X. Y. Gao², Y. Gao³⁹, Z. Gao⁴⁵, I. Garzia^{21A}, C. Geng⁴⁵, K. Goetzen¹⁰,
W. X. Gong¹, W. Gradl²², M. Greco^{48A,48C}, M. H. Gu¹, Y. T. Gu¹², Y. H. Guan¹, A. Q. Guo¹,
L. B. Guo²⁸, Y. Guo¹, Y. P. Guo²², Z. Haddadi²⁵, A. Hafner²², S. Han⁵⁰, Y. L. Han¹, X. Q. Hao¹⁵,
F. A. Harris⁴², K. L. He¹, Z. Y. He³⁰, T. Held⁴, Y. K. Heng¹, Z. L. Hou¹, C. Hu²⁸, H. M. Hu¹,
J. F. Hu^{48A,48C}, T. Hu¹, Y. Hu¹, G. M. Huang⁶, G. S. Huang⁴⁵, H. P. Huang⁵⁰, J. S. Huang¹⁵,
X. T. Huang³³, Y. Huang²⁹, T. Hussain⁴⁷, Q. Ji¹, Q. P. Ji³⁰, X. B. Ji¹, X. L. Ji¹, L. L. Jiang¹,
L. W. Jiang⁵⁰, X. S. Jiang¹, J. B. Jiao³³, Z. Jiao¹⁷, D. P. Jin¹, S. Jin¹, T. Johansson⁴⁹, A. Julin⁴³,
N. Kalantar-Nayestanaki²⁵, X. L. Kang¹, X. S. Kang³⁰, M. Kavatsyuk²⁵, B. C. Ke⁵, R. Kliemt¹⁴,
B. Kloss²², O. B. Kolcu^{40B,d}, B. Kopf⁴, M. Kornicer⁴², W. Kühn²⁴, A. Kupsc⁴⁹, W. Lai¹, J. S. Lange²⁴,
M. Lara¹⁹, P. Larin¹⁴, C. Leng^{48C}, C. H. Li¹, Cheng Li⁴⁵, D. M. Li⁵², F. Li¹, G. Li¹, H. B. Li¹, J. C. Li¹,
Jin Li³², K. Li¹³, K. Li³³, Lei Li³, P. R. Li⁴¹, T. Li³³, W. D. Li¹, W. G. Li¹, X. L. Li³³, X. M. Li¹²,
X. N. Li¹, X. Q. Li³⁰, Z. B. Li³⁸, H. Liang⁴⁵, Y. F. Liang³⁶, Y. T. Liang²⁴, G. R. Liao¹¹, D. X. Lin¹⁴,
B. J. Liu¹, C. X. Liu¹, F. H. Liu³⁵, Fang Liu¹, Feng Liu⁶, H. B. Liu¹², H. H. Liu¹, H. H. Liu¹⁶, H. M. Liu¹,
J. Liu¹, J. P. Liu⁵⁰, J. Y. Liu¹, K. Liu³⁹, K. Y. Liu²⁷, L. D. Liu³¹, P. L. Liu¹, Q. Liu⁴¹, S. B. Liu⁴⁵,
X. Liu²⁶, X. X. Liu⁴¹, Y. B. Liu³⁰, Z. A. Liu¹, Zhiqiang Liu¹, Zhiqing Liu²², H. Loehner²⁵, X. C. Lou^{1,e},
H. J. Lu¹⁷, J. G. Lu¹, R. Q. Lu¹⁸, Y. Lu¹, Y. P. Lu¹, C. L. Luo²⁸, M. X. Luo⁵¹, T. Luo⁴², X. L. Luo¹,
M. Lv¹, X. R. Lyu⁴¹, F. C. Ma²⁷, H. L. Ma¹, L. L. Ma³³, Q. M. Ma¹, S. Ma¹, T. Ma¹, X. N. Ma³⁰,
X. Y. Ma¹, F. E. Maas¹⁴, M. Maggiora^{48A,48C}, Q. A. Malik⁴⁷, Y. J. Mao³¹, Z. P. Mao¹, S. Marcello^{48A,48C},
J. G. Messchendorp²⁵, J. Min¹, T. J. Min¹, R. E. Mitchell¹⁹, X. H. Mo¹, Y. J. Mo⁶, C. Morales Morales¹⁴,
K. Moriya¹⁹, N. Yu. Muchnoi^{9,a}, H. Muramatsu⁴³, Y. Nefedov²³, F. Nerling¹⁴, I. B. Nikolaev^{9,a}, Z. Ning¹,
S. Nisar⁸, S. L. Niu¹, X. Y. Niu¹, S. L. Olsen³², Q. Ouyang¹, S. Pacetti^{20B}, P. Patteri^{20A}, M. Pelizaeus⁴,
H. P. Peng⁴⁵, K. Peters¹⁰, J. Pettersson⁴⁹, J. L. Ping²⁸, R. G. Ping¹, R. Poling⁴³, Y. N. Pu¹⁸, M. Qi²⁹,
S. Qian¹, C. F. Qiao⁴¹, L. Q. Qin³³, N. Qin⁵⁰, X. S. Qin¹, Y. Qin³¹, Z. H. Qin¹, J. F. Qiu¹,
K. H. Rashid⁴⁷, C. F. Redmer²², H. L. Ren¹⁸, M. Ripka²², G. Rong¹, X. D. Ruan¹², V. Santoro^{21A},
A. Sarantsev^{23,f}, M. Savrie^{21B}, K. Schoenning⁴⁹, S. Schumann²², W. Shan³¹, M. Shao⁴⁵, C. P. Shen²,
P. X. Shen³⁰, X. Y. Shen¹, H. Y. Sheng¹, W. M. Song¹, X. Y. Song¹, S. Sosio^{48A,48C}, S. Spataro^{48A,48C},
G. X. Sun¹, J. F. Sun¹⁵, S. S. Sun¹, Y. J. Sun⁴⁵, Y. Z. Sun¹, Z. J. Sun¹, Z. T. Sun¹⁹, C. J. Tang³⁶,
X. Tang¹, I. Tapan^{40C}, E. H. Thorndike⁴⁴, M. Tiemens²⁵, D. Toth⁴³, M. Ullrich²⁴, I. Uman^{40B},
G. S. Varner⁴², B. Wang³⁰, B. L. Wang⁴¹, D. Wang³¹, D. Y. Wang³¹, K. Wang¹, L. L. Wang¹,
L. S. Wang¹, M. Wang³³, P. Wang¹, P. L. Wang¹, Q. J. Wang¹, S. G. Wang³¹, W. Wang¹, X. F. Wang³⁹,
Y. D. Wang^{20A}, Y. F. Wang¹, Y. Q. Wang²², Z. Wang¹, Z. G. Wang¹, Z. H. Wang⁴⁵, Z. Y. Wang¹,
T. Weber²², D. H. Wei¹¹, J. B. Wei³¹, P. Weidenkaff²², S. P. Wen¹, U. Wiedner⁴, M. Wolke⁴⁹, L. H. Wu¹,
Z. Wu¹, L. G. Xia³⁹, Y. Xia¹⁸, D. Xiao¹, Z. J. Xiao²⁸, Y. G. Xie¹, Q. L. Xiu¹, G. F. Xu¹, L. Xu¹,
Q. J. Xu¹³, Q. N. Xu⁴¹, X. P. Xu³⁷, L. Yan⁴⁵, W. B. Yan⁴⁵, W. C. Yan⁴⁵, Y. H. Yan¹⁸, H. X. Yang¹,
L. Yang⁵⁰, Y. Yang⁶, Y. X. Yang¹¹, H. Ye¹, M. Ye¹, M. H. Ye⁷, J. H. Yin¹, B. X. Yu¹, C. X. Yu³⁰,
H. W. Yu³¹, J. S. Yu²⁶, C. Z. Yuan¹, W. L. Yuan²⁹, Y. Yuan¹, A. Yuncu^{40B,g}, A. A. Zafar⁴⁷, A. Zallo^{20A},
Y. Zeng¹⁸, B. X. Zhang¹, B. Y. Zhang¹, C. Zhang²⁹, C. C. Zhang¹, D. H. Zhang¹, H. H. Zhang³⁸,
H. Y. Zhang¹, J. J. Zhang¹, J. L. Zhang¹, J. Q. Zhang¹, J. W. Zhang¹, J. Y. Zhang¹, J. Z. Zhang¹,
K. Zhang¹, L. Zhang¹, S. H. Zhang¹, X. Y. Zhang³³, Y. Zhang¹, Y. H. Zhang¹, Y. T. Zhang⁴⁵,

Z. H. Zhang⁶, Z. P. Zhang⁴⁵, Z. Y. Zhang⁵⁰, G. Zhao¹, J. W. Zhao¹, J. Y. Zhao¹, J. Z. Zhao¹, Lei Zhao⁴⁵,
Ling Zhao¹, M. G. Zhao³⁰, Q. Zhao¹, Q. W. Zhao¹, S. J. Zhao⁵², T. C. Zhao¹, Y. B. Zhao¹, Z. G. Zhao⁴⁵,
A. Zhemchugov^{23,h}, B. Zheng⁴⁶, J. P. Zheng¹, W. J. Zheng³³, Y. H. Zheng⁴¹, B. Zhong²⁸, L. Zhou¹,
Li Zhou³⁰, X. Zhou⁵⁰, X. K. Zhou⁴⁵, X. R. Zhou⁴⁵, X. Y. Zhou¹, K. Zhu¹, K. J. Zhu¹, S. Zhu¹,
X. L. Zhu³⁹, Y. C. Zhu⁴⁵, Y. S. Zhu¹, Z. A. Zhu¹, J. Zhuang¹, L. Zotti^{48A,48C}, B. S. Zou¹, J. H. Zou¹

(BESIII Collaboration)

- ¹ *Institute of High Energy Physics, Beijing 100049, People's Republic of China*
² *Beihang University, Beijing 100191, People's Republic of China*
³ *Beijing Institute of Petrochemical Technology, Beijing 102617, People's Republic of China*
⁴ *Bochum Ruhr-University, D-44780 Bochum, Germany*
⁵ *Carnegie Mellon University, Pittsburgh, Pennsylvania 15213, USA*
⁶ *Central China Normal University, Wuhan 430079, People's Republic of China*
⁷ *China Center of Advanced Science and Technology, Beijing 100190, People's Republic of China*
⁸ *COMSATS Institute of Information Technology, Lahore, Defence Road, Off Raiwind Road, 54000
Lahore, Pakistan*
⁹ *G.I. Budker Institute of Nuclear Physics SB RAS (BINP), Novosibirsk 630090, Russia*
¹⁰ *GSI Helmholtzcentre for Heavy Ion Research GmbH, D-64291 Darmstadt, Germany*
¹¹ *Guangxi Normal University, Guilin 541004, People's Republic of China*
¹² *GuangXi University, Nanning 530004, People's Republic of China*
¹³ *Hangzhou Normal University, Hangzhou 310036, People's Republic of China*
¹⁴ *Helmholtz Institute Mainz, Johann-Joachim-Becher-Weg 45, D-55099 Mainz, Germany*
¹⁵ *Henan Normal University, Xinxiang 453007, People's Republic of China*
¹⁶ *Henan University of Science and Technology, Luoyang 471003, People's Republic of China*
¹⁷ *Huangshan College, Huangshan 245000, People's Republic of China*
¹⁸ *Hunan University, Changsha 410082, People's Republic of China*
¹⁹ *Indiana University, Bloomington, Indiana 47405, USA*
²⁰ *(A)INFN Laboratori Nazionali di Frascati, I-00044, Frascati, Italy; (B)INFN and University of Perugia,
I-06100, Perugia, Italy*
²¹ *(A)INFN Sezione di Ferrara, I-44122, Ferrara, Italy; (B)University of Ferrara, I-44122, Ferrara, Italy*
²² *Johannes Gutenberg University of Mainz, Johann-Joachim-Becher-Weg 45, D-55099 Mainz, Germany*
²³ *Joint Institute for Nuclear Research, 141980 Dubna, Moscow region, Russia*
²⁴ *Justus Liebig University Giessen, II. Physikalisches Institut, Heinrich-Buff-Ring 16, D-35392 Giessen,
Germany*
²⁵ *KVI-CART, University of Groningen, NL-9747 AA Groningen, The Netherlands*
²⁶ *Lanzhou University, Lanzhou 730000, People's Republic of China*
²⁷ *Liaoning University, Shenyang 110036, People's Republic of China*
²⁸ *Nanjing Normal University, Nanjing 210023, People's Republic of China*
²⁹ *Nanjing University, Nanjing 210093, People's Republic of China*
³⁰ *Nankai University, Tianjin 300071, People's Republic of China*
³¹ *Peking University, Beijing 100871, People's Republic of China*
³² *Seoul National University, Seoul, 151-747 Korea*
³³ *Shandong University, Jinan 250100, People's Republic of China*
³⁴ *Shanghai Jiao Tong University, Shanghai 200240, People's Republic of China*
³⁵ *Shanxi University, Taiyuan 030006, People's Republic of China*
³⁶ *Sichuan University, Chengdu 610064, People's Republic of China*
³⁷ *Soochow University, Suzhou 215006, People's Republic of China*
³⁸ *Sun Yat-Sen University, Guangzhou 510275, People's Republic of China*
³⁹ *Tsinghua University, Beijing 100084, People's Republic of China*
⁴⁰ *(A)Istanbul Aydin University, 34295 Sefakoy, Istanbul, Turkey; (B)Dogus University, 34722 Istanbul,
Turkey; (C)Uludag University, 16059 Bursa, Turkey*
⁴¹ *University of Chinese Academy of Sciences, Beijing 100049, People's Republic of China*

- ⁴² University of Hawaii, Honolulu, Hawaii 96822, USA
⁴³ University of Minnesota, Minneapolis, Minnesota 55455, USA
⁴⁴ University of Rochester, Rochester, New York 14627, USA
⁴⁵ University of Science and Technology of China, Hefei 230026, People's Republic of China
⁴⁶ University of South China, Hengyang 421001, People's Republic of China
⁴⁷ University of the Punjab, Lahore-54590, Pakistan
⁴⁸ (A)University of Turin, I-10125, Turin, Italy; (B)University of Eastern Piedmont, I-15121, Alessandria, Italy; (C)INFN, I-10125, Turin, Italy
⁴⁹ Uppsala University, Box 516, SE-75120 Uppsala, Sweden
⁵⁰ Wuhan University, Wuhan 430072, People's Republic of China
⁵¹ Zhejiang University, Hangzhou 310027, People's Republic of China
⁵² Zhengzhou University, Zhengzhou 450001, People's Republic of China
^a Also at the Novosibirsk State University, Novosibirsk, 630090, Russia
^b Also at Ankara University, 06100 Tandogan, Ankara, Turkey
^c Also at the Moscow Institute of Physics and Technology, Moscow 141700, Russia and at the Functional Electronics Laboratory, Tomsk State University, Tomsk, 634050, Russia
^d Currently at Istanbul Arel University, 34295 Istanbul, Turkey
^e Also at University of Texas at Dallas, Richardson, Texas 75083, USA
^f Also at the NRC "Kurchatov Institute", PNPI, 188300, Gatchina, Russia
^g Also at Bogazici University, 34342 Istanbul, Turkey
^h Also at the Moscow Institute of Physics and Technology, Moscow 141700, Russia

Abstract

Using the data sets taken at center-of-mass energies above 4 GeV by the BESIII detector at the BEPCII storage ring, we search for the reaction $e^+e^- \rightarrow \gamma_{\text{ISR}} X(3872) \rightarrow \gamma_{\text{ISR}} \pi^+ \pi^- J/\psi$ via the Initial State Radiation technique. The production of a resonance with quantum numbers $J^{PC} = 1^{++}$ such as the $X(3872)$ via single photon e^+e^- annihilation is forbidden, but is allowed by a next-to-leading order box diagram. We do not observe a significant signal of $X(3872)$, and therefore give an upper limit for the electronic width times the branching fraction $\Gamma_{ee}^{X(3872)} \mathcal{B}(X(3872) \rightarrow \pi^+ \pi^- J/\psi) < 0.13 \text{ eV}$ at the 90% confidence level. This measurement improves upon existing limits by a factor of 46. Using the same final state, we also measure the electronic width of the $\psi(3686)$ to be $\Gamma_{ee}^{\psi(3686)} = 2213 \pm 18_{\text{stat}} \pm 99_{\text{sys}} \text{ eV}$.

Keywords: $X(3872)$, $\psi(3686)$, Γ_{ee} , charmonium spectroscopy, BESIII

1. Introduction

2 The $X(3872)$ resonance was observed in 2003 by
3 Belle [1] in the decay channel $\pi^+ \pi^- J/\psi$. The ex-
4 istence of this state was later confirmed by several
5 other experiments [2, 3, 4, 5, 6]. The observation
6 of the decay channel $X(3872) \rightarrow \gamma J/\psi$ implies that
7 the state has even C-parity [5, 7, 8]. The quantum
8 numbers were finally determined to be $J^{PC} = 1^{++}$
9 [5, 9]. However, the intrinsic nature of the reso-
10 nance is still unknown and has led to many con-
11 jectures. It is a good candidate for a tetraquark

12 state but also for a meson molecule as its mass
13 is close to the $D^0 \bar{D}^{*0}$ threshold [10]. The recent
14 observation of the decay $Y(4260) \rightarrow \gamma X(3872)$ by
15 BESIII [6] implies that the $X(3872)$ could be a me-
16 son molecule, as suggested by a model dependent
17 calculation [11]. On the other hand, the large decay
18 rate of $X(3872) \rightarrow \gamma \psi(3686)$ observed by BaBar
19 and LHCb, compared to $X(3872) \rightarrow \gamma J/\psi$ hints
20 at a tetraquark state explanation [8, 12, 13]. One
21 of the interesting quantities, which may help to re-
22 veal the structure of the $X(3872)$ is its electronic

width Γ_{ee} . A recent order-of-magnitude calculation using a Vector Meson Dominance model predicts $\Gamma_{ee}^{X(3872)} \approx 0.03$ eV [14], without any prior assumption regarding the nature of the $X(3872)$. For comparison, calculations for the Γ_{ee} of the ordinary 1^{++} charmonium state χ_{c1} have been carried out [15] and the electronic width is found to be in the range between 0.044 eV and 0.46 eV. This was also confirmed in a more recent calculation [14].

The current upper limit for $\Gamma_{ee}^{X(3872)}$ is at the $\mathcal{O}(10^2)$ eV level [16], which is three orders of magnitude larger than the theoretical prediction. The aim of this work is to obtain a significantly improved experimental value for the electronic width of $X(3872)$ that may be contrasted with predictions of Γ_{ee} within various theoretical models making different assumptions regarding the nature of the $X(3872)$.

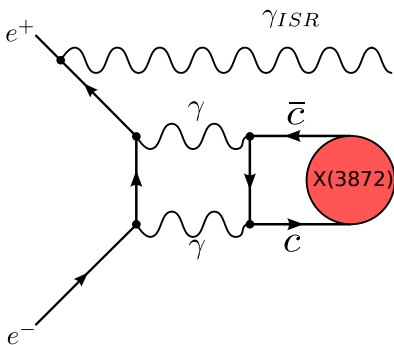


Figure 1: ISR production of $X(3872)$ via a box diagram.

The production of a 1^{++} resonance has never been observed in e^+e^- annihilation so far. Such a process may occur via a two-photon box diagram as depicted in Fig. 1. In order to search for a possible signal we analyze data taken by the BESIII detector at center-of-mass (c.m.) energies above 3.872 GeV, using the Initial State Radiation (ISR) technique. The ISR photon reduces the available c.m. energy, such that the $X(3872)$ can be produced resonantly via the two-photon process. In the process $e^+e^- \rightarrow \gamma_{\text{ISR}}X(3872)$ we search for the $X(3872)$ in its decay to $\pi^+\pi^-J/\psi$ with $J/\psi \rightarrow \ell^+\ell^-$ ($\ell = \mu$ and e). The $\pi^+\pi^-J/\psi$ mass spectrum is expected to be dominated by the well known process $e^+e^- \rightarrow \gamma_{\text{ISR}}\psi(3686)$.

2. BESIII Detector, Data and Monte Carlo

BESIII is a general purpose detector, covering 93% of the solid angle. It is operating at the e^+e^- double-ring collider BEPCII. A detailed description of the facilities is given in Ref. [18]. BESIII consists of four main components: (a) The helium-based 43 layer main drift chamber (MDC) provides an average single-hit resolution of $135 \mu\text{m}$, and a momentum resolution of 0.5% for charged-particle at 1 GeV/c in a 1 T magnetic field. (b) The electromagnetic calorimeter (EMC) consists of 6240 CsI(Tl) crystals, arrayed in a cylindrical structure (barrel) and two endcaps. The energy resolution for 1.0 GeV photons is 2.5% (5%) in the barrel (endcaps), while the position resolution is 6 mm (9 mm) in the barrel (endcaps). (c) The time-of-flight system (TOF) is constructed of 5 cm thick plastic scintillators and includes 88 detectors of 2.4 m length in two layers in the barrel and 96 fan-shaped detectors in the endcaps. The barrel (endcap) time resolution of 80 ps (110 ps) provides 2 sigma K/π separation for momenta up to about 1.0 GeV/c. (d) The muon counter (MUC) consists of resistive plate chambers in nine barrel and eight endcap layers. It is incorporated in the return iron of the superconducting magnet. Its position resolution is about 2 cm.

A GEANT4 [19, 20] based detector simulation package is used to model the detector response. This analysis is based on four data samples taken at c.m. energies of 4.009 GeV, 4.230 GeV, 4.260 GeV and 4.360 GeV by the BESIII detector. The integrated luminosity of each data sample is listed in Table 1. The total integrated luminosity is $\mathcal{L}_{\text{tot}} = 2.94 \text{ fb}^{-1}$. We simulate the $e^+e^- \rightarrow X(3872)\gamma_{\text{ISR}}$ signal process using EVTGEN [21, 22], which invokes the VECTORISR generator model [23] for the ISR process and the common $\rho J/\psi$ model for the decay $X(3872) \rightarrow \pi^+\pi^-J/\psi$. The Monte Carlo (MC) simulation of the $e^+e^- \rightarrow \gamma_{\text{ISR}}\psi(3686)$ process was performed using the PHOKHARA generator [24]. For the background study we simulate the $e^+e^- \rightarrow \eta J/\psi$ process with EVTGEN and the $e^+e^- \rightarrow \gamma_{\text{ISR}}\pi^+\pi^-\pi^+\pi^-$ process with PHOKHARA.

3. Event Selection

For the event selection, we require four charged tracks with net charge zero. The point of closest approach to the e^+e^- interaction point is required to be within ± 10 cm in the beam direction and 1 cm in the plane perpendicular to the

106 beam direction. As the J/ψ resonance carries
 108 most of the total momentum, the final state lep-
 110 tons can be distinguished from pions by their mo-
 112 menta in the lab frame. Tracks with momen-
 114 tum $p > 1 \text{ GeV}/c$ in the lab frame are identified
 116 as leptons, whereas tracks with $p < 600 \text{ MeV}/c$
 118 are identified as pions. The particle identification
 120 for leptons is achieved by measuring the ratio of
 122 the energy deposited in the EMC divided by the
 124 track's momentum measured in the MDC (E/p).
 126 If $E/p > 0.4$, we assume the lepton to be an
 128 electron, otherwise it is considered a muon candi-
 130 date. The E/p distributions of data and MC agree
 132 well, and MC studies show that the background for
 134 $J/\psi \rightarrow e^+e^-$ is negligible. The resolution of the in-
 136 variant mass of the lepton pairs is $16 \text{ MeV}/c^2$. We
 138 require their invariant mass $M(\ell^+\ell^-)$ to be within
 140 $3.05 \leq M(\ell^+\ell^-) \leq 3.14 \text{ GeV}/c^2$ for the J/ψ signal
 142 selection. Furthermore the opening angle between
 144 the two pion tracks is required to satisfy $\cos \alpha_{\pi\pi} \leq$
 146 0.6 to remove background from $e^+e^- \rightarrow \eta J/\psi$ as
 148 well as background from mis-identified electrons
 150 which originate from γ -conversion. Due to the
 152 boost of the η meson in the laboratory frame, the
 154 opening angles of its decay products are small. The
 reaction $e^+e^- \rightarrow \gamma X(3872)$ recently observed by
 BESIII [6], where the photon comes from a radiative
 transition of the $Y(4260)$, represents an irre-
 ducible background to our signal process. To avoid
 this background, the ISR photon is required to be
 emitted at small polar angles $|\cos \theta_{\text{ISR}}| > 0.95$, al-
 most colinear to the beam direction. Since the ISR
 photon cannot be detected in this region of the de-
 tector, its energy and polar angle are calculated
 from the missing momentum of the event (untagged
 ISR photon). As the photon from the radiative de-
 cay channel is predominantly emitted at large po-
 lar angles, an optimal signal to background ratio
 is obtained in this way. An MC simulation study
 shows that the $Y(4260) \rightarrow \gamma X(3872)$ background
 can be neglected in the region of small polar an-
 gles of the ISR photon. To improve the resolution
 of the $\pi^+\pi^- J/\psi$ mass spectrum and to further re-
 move background, a two-constraint (2C) kinematic
 fit under the hypothesis of the $\gamma_{\text{ISR}}\pi^+\pi^-\ell^+\ell^-$ final
 state is performed. The two constraints are the J/ψ
 mass for the lepton pair and the mass of the missing
 ISR photon, which is zero. We accept events with
 $\chi_{2C}^2 < 15$.

4. $\pi^+\pi^- J/\psi$ Mass Spectrum

156 The invariant mass distributions of
 158 $M(\pi^+\pi^- J/\psi)$ for data, signal simulation, and sim-
 160 ulation of the dominant background $e^+e^- \rightarrow \eta J/\psi$
 162 are shown in Fig. 2. All the selection criteria
 164 described above have been applied here. As ex-
 166 pected, the mass spectrum is dominated by the
 168 $\psi(3686)$ resonance. No significant $X(3872)$ peak is
 170 observed at any of the four c.m. energies. Hence,
 172 we set an upper limit for the electronic width of
 $X(3872)$. In Fig. 2, the blue dotted histogram rep-
 resents the signal simulation of the $X(3872)$ with
 arbitrary normalization. The background channels
 of $e^+e^- \rightarrow \pi^+\pi^-\pi^+\pi^-\gamma_{\text{ISR}}$ and $e^+e^- \rightarrow \eta' J/\psi$
 with $\eta' \rightarrow \gamma\pi^+\pi^-$ are found to be negligible in
 an MC simulation study. The background channel
 $e^+e^- \rightarrow \eta J/\psi$ with $\eta \rightarrow \pi^+\pi^-\pi^0$ is displayed as
 the orange dashed-dotted line in Fig. 2.

174 Unbinned maximum likelihood fits are per-
 176 formed to extract the yields of $\psi(3686)$ and
 $X(3872)$ events at each c.m. energy, where the line
 shapes of background are represented by polyno-
 mial functions and the line shapes of $\psi(3686)$ and
 $X(3872)$ are described by the MC shape convoluted
 with a Gaussian function which takes into account
 resolution differences between data and MC simula-
 tion. We use the same parameters of the Gaussian
 function for the two resonances. The fit results are
 displayed as the solid red curves in Fig. 2. The
 event yields of $\psi(3686)$ from the fits are shown in
 Table 1.

5. Calculation of Γ_{ee}

186 The measured radiative event yield N_A of the
 188 process $e^+e^- \rightarrow \gamma_{\text{ISR}} A$ can be expressed as a func-
 tion of $x \equiv 1 - \frac{M(\pi^+\pi^- J/\psi)^2}{s}$ [25]:

$$\frac{dN_A}{dx} = W(s, x) \varepsilon_A \mathcal{L} \sigma(e^+e^- \rightarrow A) \mathcal{B}(A \rightarrow f), \quad (1)$$

190 where s is the squared c.m. energy, $W(s, x)$ de-
 192 notes the radiator function, ε_A is the corre-
 194 sponding reconstruction efficiency, \mathcal{L} is the in-
 196 tegrated luminosity, $\sigma(e^+e^- \rightarrow A)$ is the Born
 cross section to produce A in e^+e^- annihilation,
 $\mathcal{B}(A \rightarrow f) = \mathcal{B}(A \rightarrow \pi^+\pi^- J/\psi) \mathcal{B}(J/\psi \rightarrow \ell^+\ell^-)$ is
 the product of the branching fractions of A decay-
 ing into the final state f .

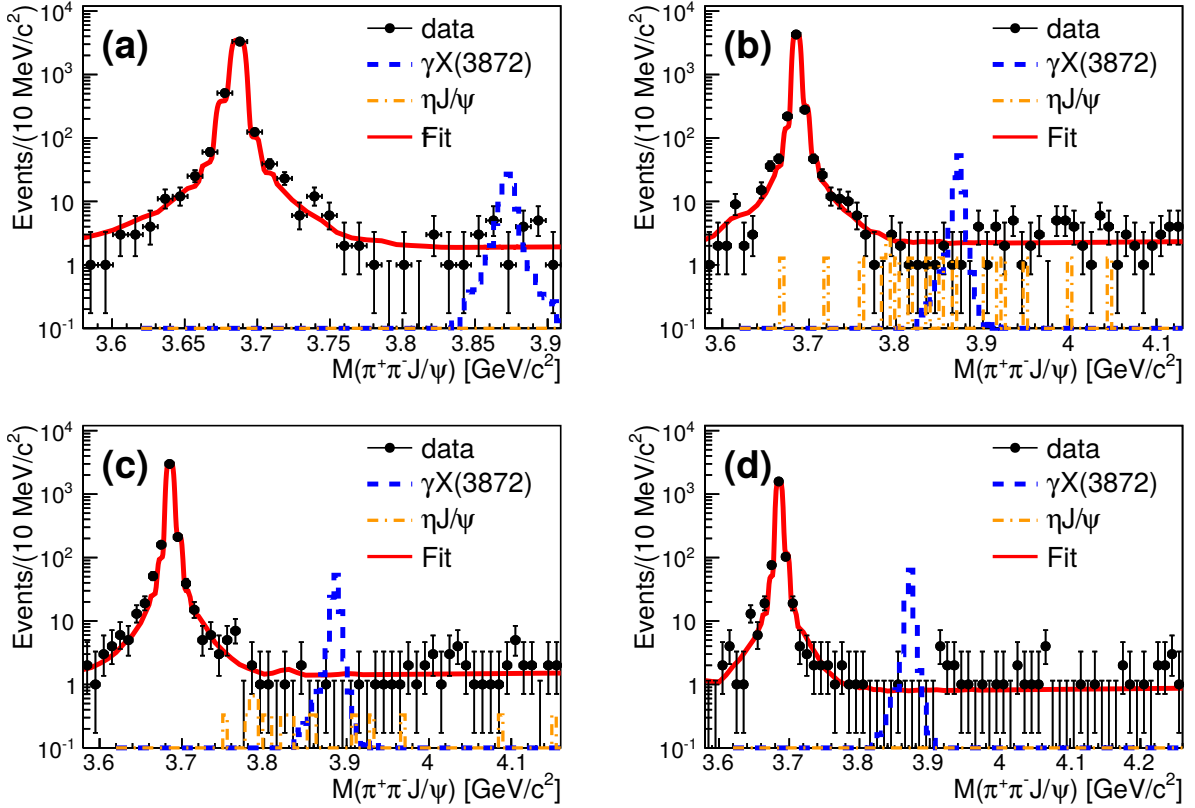


Figure 2: The $\pi^+\pi^-J/\psi$ mass distributions at (a) $\sqrt{s} = 4.009$ GeV, (b) 4.230 GeV, (c) 4.260 GeV and (d) 4.360 GeV. Dots with error bars are data, the solid red lines are the fit curves, the blue dashed histograms are MC simulated $X(3872)$ signal events, which are normalized arbitrarily, and the orange dot-dashed histograms are MC simulated $\eta J/\psi$ background events.

198 The relationship between the electronic width
 Γ_{ee} and the Born cross section reads:

$$\sigma(e^+e^- \rightarrow A) = \frac{12\pi\Gamma_{ee}\Gamma_{\text{tot}}}{(s' - M_A^2)^2 + \Gamma_{\text{tot}}^2 M_A^2}, \quad (2)$$

200 where $s' = (1 - x)s$, Γ_{ee} (Γ_{tot}) is the electronic
 (total) width of the resonance A , and M_A is its
 202 mass. Eq. (1) must be integrated over s' in an
 appropriate region around the resonance A . The
 204 integral only involves the Breit-Wigner function in
 the Born cross section and the radiator function.
 206 Hence it can be separated from the quantities deter-
 mined in the measurement, such that the integral
 208 enters the calculation of the electronic width
 as a factor denoted by I_A . This factor is given by
 210 $I_A = 12\pi\Gamma_{\text{tot}} \int_{x_1}^{x_2} dx \frac{W(s,x)}{(s' - M_A^2)^2 + \Gamma_{\text{tot}}^2 M_A^2}$. The limits of
 the integral are chosen to coincide with the signal
 212 region.

214 Using Eq. (1), the electronic width times the
 branching fraction $\mathcal{B}(A \rightarrow \pi^+\pi^-J/\psi)$ can then be
 obtained via the relation

$$\Gamma_{ee}^A \mathcal{B}(A \rightarrow \pi^+\pi^-J/\psi) = \frac{N_A}{\varepsilon_A \mathcal{L} I_A \mathcal{B}(J/\psi \rightarrow \ell^+\ell^-)}, \quad (3)$$

216 which is used to determine the electronic widths
 of $X(3872)$ and $\psi(3686)$. As no significant signal
 218 is found in the case of $X(3872)$, we calcu-
 late an upper limit for $\Gamma_{ee}^{X(3872)}$. For the branch-
 220 ing fractions we take the latest BESIII values
 $\mathcal{B}(\psi(3686) \rightarrow \pi^+\pi^-J/\psi) = (34.98 \pm 0.45)\%$ and
 222 $\mathcal{B}(J/\psi \rightarrow \ell^+\ell^-) = (11.96 \pm 0.05)\%$ [26]. The
 reconstruction efficiencies ε_A are extracted from
 224 the signal MC sample $e^+e^- \rightarrow \gamma_{\text{ISR}} X(3872)$ and
 $e^+e^- \rightarrow \gamma_{\text{ISR}} \psi(3686)$, respectively. We apply an
 226 additional relative correction factor of 2%, which
 stems from a data-MC difference found in the χ^2

Table 1: Values for the integrals ($I_{\psi(3686)}$ and $I_{X(3872)}$), the efficiencies ($\epsilon_{\psi(3686)}$ and $\epsilon_{X(3872)}$), the event yield $N_{\psi(3686)}^{obs}$ and the electronic widths ($\Gamma_{ee}^{\psi(3686)}$ and $\Gamma_{ee}^{X(3872)}\mathcal{B}(X(3872) \rightarrow \pi^+\pi^-J/\psi)$). The errors shown are statistical only.

c.m. energy [GeV]	4.009	4.230	4.260	4.360
\mathcal{L} [pb $^{-1}$]	482	1092	826	540
$I_{\psi(3686)}$ [pb/keV]	310	172	161	133
$I_{X(3872)}$ [pb/keV]	671	247	225	174
$\epsilon_{\psi(3686)}$	0.303	0.286	0.286	0.282
$\epsilon_{X(3872)}$	0.314	0.324	0.325	0.327
$N^{\psi(2S)}$	4168 \pm 65	5026 \pm 71	3547 \pm 60	1846 \pm 43
$\Gamma_{ee}^{\psi(3686)}$ [eV]	2198 \pm 34	2232 \pm 32	2223 \pm 38	2176 \pm 51
$\Gamma_{ee}^{X(3872)}\mathcal{B}(X(3872) \rightarrow \pi^+\pi^-J/\psi)$ at 90% C.L. [eV]	0.630	0.314	0.319	0.646

distributions. To obtain this correction factor, the number of events in the background-free $\psi(3686)$ mass region ($3.62 < M(\pi^+\pi^-J/\psi) < 3.75$ GeV/ c^2) passing the $\chi_{2C}^2 < 15$ requirement relative to all reconstructed events in MC is compared to the respective number obtained from data. All the values for the efficiencies and the integrals I_A at each c.m. energy point are listed in Table 1. The statistical errors of the efficiencies are negligible. First we compute the electronic width of $\psi(3686)$, which is denoted by $\Gamma_{ee}^{\psi(3686)}$. This serves as a benchmark and validation of our method, since the electronic width of $\psi(3686)$ is already known with high accuracy [16]. Applying the numbers for $\psi(3686)$ listed in Table 1 to Eq. (3), we obtain the value for $\Gamma_{ee}^{\psi(3686)}$ at each of the four energy points separately, as shown in Table 1. We calculate the error weighted average of the electronic width of $\psi(3686)$ from the four single measurements in Table 1, which gives $\Gamma_{ee}^{\psi(3686)} = (2213 \pm 18_{\text{stat}})$ eV.

Since no $X(3872)$ signal is observed, we set an upper limit at the 90% confidence level (C.L.) for its electronic width. Applying the Bayesian method, we perform likelihood scans at each of the four data sets of the electronic width times the branching fraction, which is proportional to the $X(3872)$ event yield parameter N_i according to Eq. (3). This provides four likelihood curves, that are denoted by $L_i(\gamma)$, $i = 1 \dots 4$, where $\gamma = \Gamma_{ee}^{X(3872)}\mathcal{B}(X(3872) \rightarrow \pi^+\pi^-J/\psi)$. We look for the values γ_i^{up} that yield 90% of the likelihood integral over γ from zero to infinity: $\int_0^{\gamma_i^{\text{up}}} d\gamma L_i(\gamma) = 0.9 \int_0^\infty d\gamma L_i(\gamma)$. In order to combine the four measurements, we construct the like-

lihood of the combined measurement. The four single likelihood curves are scaled such that they have the same value at their respective maxima. We take the product of the likelihood scan curves of the single measurements. The upper limit $\gamma_{\text{tot}}^{\text{up}}$ at the 90% C.L. of γ is determined from

$$\int_0^{\gamma_{\text{tot}}^{\text{up}}} d\gamma \prod_{i=1}^4 L_i(\gamma) = 0.9 \int_0^\infty d\gamma \prod_{i=1}^4 L_i(\gamma),$$

We obtain $\gamma_{\text{tot}}^{\text{up}} = \Gamma_{ee}^{X(3872)}\mathcal{B}(X(3872) \rightarrow \pi^+\pi^-J/\psi) = 0.125$ eV at the 90% C.L.

6. Estimation of Systematic Uncertainties

The luminosity is measured using large angle Bhabha events, and the uncertainty is estimated to be 1% [27]. The uncertainty related to the tracking efficiency is 1% per charged track [6]. Since the final state has four charged tracks, we estimate an uncertainty of 4% for the whole event. Applying our J/ψ selection both to data and the $\psi(3686)\gamma_{\text{ISR}}$ MC simulation, the obtained event yield differs by 0.2%, which we take as systematic uncertainty for the J/ψ selection. To correct for differences between data and MC simulation in the χ_{2C}^2 distribution, an efficiency correction was determined. Varying the χ_{2C}^2 selection and calculating the efficiency correction factor again at each energy, we obtain a corresponding uncertainty of 0.4% in the luminosity weighted average. The integrals I_A have an uncertainty of 0.7%, due to the precision of the numerical integration (0.5%) and the calculation of the radiator function (0.5%). The relative uncertainties of the

290 branching fraction $\mathcal{B}(\psi(3686) \rightarrow \pi^+\pi^- J/\psi)$ and
 292 $\mathcal{B}(J/\psi \rightarrow \ell^+\ell^-)$ are 1.3% and 0.5%, respectively. 328
 There is no correlation between these branching
 294 fractions [26]. We take 1.4% as the systematic 330
 uncertainty from the branching fractions for the
 296 electronic width of $\psi(3686)$. In the calculation of
 $\Gamma_{ee}^{X(3872)} \mathcal{B}(X(3872) \rightarrow \pi^+\pi^- J/\psi)$ only the branching
 298 fraction $\mathcal{B}(J/\psi \rightarrow \ell^+\ell^-)$ appears. Hence, the 334
 corresponding uncertainty is 0.5%. To estimate the
 300 systematic uncertainty due to the width assumed
 for $X(3872)$, we change the width by $\pm 0.2 \text{ MeV}/c^2$
 302 and repeat the entire fitting procedure. The maxi-
 mal relative difference of these results from the re-
 304 sult obtained with the standard width is found to
 be 2.7% in the luminosity-weighted average. The
 306 detection efficiency of ISR $X(3872)$ events was de-
 termined from a MC simulation using the VEC-
 308 TORISR model [23], since this final state is not avail-
 able in the PHOKHARA event generator. On the
 310 other hand, the ISR $\psi(3686)$ detection efficiency
 was determined using the PHOKHARA event gener-
 312 ator, which simulates ISR events with 0.5% preci-
 sion. To obtain the uncertainty of the ISR simula-
 314 tion with the VECTORISR model, we compare the ef-
 ficiencies of ISR $\psi(3686)$ events generated with the
 PHOKHARA event generator [24] and the VECTORISR
 316 module [23]. The luminosity-weighted average dif-
 ference is found to be 3.4% between them, which is
 318 taken as systematic uncertainty for the VECTORISR
 model.

Table 2: Sources of systematic uncertainties and their contribution (%).

Source	$\sigma_{\text{sys}}^{X(3872)}$	$\sigma_{\text{sys}}^{\psi(3686)}$
Luminosity	1.0	1.0
Tracking	4.0	4.0
J/ψ selection	0.2	0.2
Kinematic Fit	0.4	0.4
Integrals I_A	0.7	0.7
Branching ratio	0.5	1.4
$X(3872)$ width	2.7	-
ISR simulation	3.4	-
$\psi(3686)$ fit model	-	1.0
Total	6.1	4.5

322 For $\Gamma_{ee}^{\psi(3686)}$ a further systematic uncertainty oc-
 curs due to the choice of the fit function. In order to
 324 deal with this uncertainty, we determine the num-
 ber of $N_{\psi(3686)}^{\text{MC}}$ using a second fit function, which
 326 is a double Gaussian for the $\psi(3686)$ peak plus a
 Gaussian for the $X(3872)$ plus a constant for back-

ground. In the luminosity-weighted average, this
 fit model differs by 1.0%, which is taken as system-
 atic uncertainty. Signal events with a hard final
 state radiation (FSR) photon are rejected since the
 J/ψ mass is constraint in the kinematic fit. Thus
 FSR effects are negligible. Systematic uncertainties
 from the background shape and the fit range have
 been found to be negligible. The full list of system-
 atic uncertainties is shown in Table 2. Assuming
 the sources to be independent, the total systematic
 uncertainty for the electronic width of $X(3872)$ is
 6.1%, while in the case of $\psi(3686)$ we find a sys-
 tematic uncertainty of 4.5%.

7. Summary

We have performed a search of the process
 $e^+e^- \rightarrow \gamma_{\text{ISR}} X(3872) \rightarrow \gamma_{\text{ISR}} \pi^+\pi^- J/\psi$ using the
 ISR untagged method, where the production of
 $X(3872)$ in e^+e^- annihilations is possible via a two-
 photon box diagram. No significant $X(3872)$ signal
 is observed in the $\pi^+\pi^- J/\psi$ mass spectrum. We set
 an upper limit for the electronic width of $X(3872)$.
 By combining all four data sets, we finally obtain

$$\Gamma_{ee}^{X(3872)} \mathcal{B}(X(3872) \rightarrow \pi^+\pi^- J/\psi) < 0.13 \text{ eV}$$

at the 90% C.L. Here we have multiplied the
 upper limit by a factor $1/(1 - \sigma_{\text{sys}})$ in order
 to take the systematic uncertainties into account.
 Our measurement improves upon the current limit
 $\Gamma_{ee}^{X(3872)} \mathcal{B}(X(3872) \rightarrow \pi^+\pi^- J/\psi) < 6.2 \text{ eV}$ at the
 90% C.L. [17] by a factor of 46. If we assume the
 branching fraction $\mathcal{B}(X(3872) \rightarrow \pi^+\pi^- J/\psi) > 3\%$
 [16, 28], we obtain an upper limit for the electronic
 width of $X(3872)$ to be $\Gamma_{ee}^{X(3872)} < 4.3 \text{ eV}$. For the
 first time we obtain a value for $\Gamma_{ee}^{X(3872)}$ on the
 $\mathcal{O}(\text{eV})$ level, which is the level predicted for ordi-
 nary charmonium states [15]. However, our upper
 limit is still larger than a theoretical calculation [14]
 which predicts $\Gamma_{ee} \gtrsim 0.03 \text{ eV}$. The results should
 encourage theorists to compute the electronic width
 of $X(3872)$ under different assumptions regarding
 its intrinsic nature and to confront these calcula-
 tions with our measurement. This might lead to
 new insights regarding the nature of $X(3872)$.

We have also measured the electronic width of
 the well-known $\psi(3686)$ resonance with the result:

$$\Gamma_{ee}^{\psi(3686)} = (2213 \pm 18_{\text{stat}} \pm 99_{\text{sys}}) \text{ eV}.$$

This is in agreement with the PDG [16] fit, which
 is $(2360 \pm 40) \text{ eV}$. With a similar accuracy as the

one reported in [29], this is the best individual measurement of $\Gamma_{ee}^{\psi(3686)}$ to date.

8. Acknowledgement

The BESIII collaboration thanks the staff of BEPCII and the IHEP computing center for their strong support. This work is supported in part by National Key Basic Research Program of China under Contract No. 2015CB856700; National Natural Science Foundation of China (NSFC) under Contracts Nos. 11125525, 11235011, 11322544, 11335008, 11425524; the Chinese Academy of Sciences (CAS) Large-Scale Scientific Facility Program; Joint Large-Scale Scientific Facility Funds of the NSFC and CAS under Contracts Nos. 11179007, U1232201, U1332201; CAS under Contracts Nos. KJCX2-YW-N29, KJCX2-YW-N45; 100 Tal-

ents Program of CAS; INPAC and Shanghai Key Laboratory for Particle Physics and Cosmology; German Research Foundation DFG under Contract No. CRC-1044; Seventh Framework Programme of the European Union under Marie Curie International Incoming Fellowship Grant Agreement No. 627240; Istituto Nazionale di Fisica Nucleare, Italy; Ministry of Development of Turkey under Contract No. DPT2006K-120470; Russian Foundation for Basic Research under Contract No. 14-07-91152; U. S. Department of Energy under Contracts Nos. DE-FG02-04ER41291, DE-FG02-05ER41374, DE-FG02-94ER40823, DESC0010118; U.S. National Science Foundation; University of Groningen (RuG) and the Helmholtzzentrum fuer Schwerionenforschung GmbH (GSI), Darmstadt; WCU Program of National Research Foundation of Korea under Contract No. R32-2008-000-10155-0.

References

- [1] S. K. Choi *et al.* [Belle Collaboration], Phys. Rev. Lett. **91**, 262001 (2003).
- [2] D. Acosta *et al.* [CDF Collaboration], Phys. Rev. Lett. **93**, 072001 (2004).
- [3] V. M. Abazov *et al.* [D0 Collaboration], Phys. Rev. Lett. **93**, 162002 (2004).
- [4] B. Aubert *et al.* [BaBar Collaboration], Phys. Rev. D **71**, 071103 (2005).
- [5] R. Aaij *et al.* [LHCb Collaboration], Phys. Rev. Lett. **110**, 222001 (2013).
- [6] M. Ablikim *et al.* [BESIII Collaboration], Phys. Rev. Lett. **112**, 092001 (2014).
- [7] B. Aubert *et al.* [BaBar Collaboration], Phys. Rev. D **74**, 071101 (2006).
- [8] V. Bhardwaj *et al.* [Belle Collaboration], Phys. Rev. Lett. **107**, 091803 (2011).
- [9] A. Abulencia *et al.* [CDF Collaboration], Phys. Rev. Lett. **98**, 132002 (2007).
- [10] N. Brambilla, S. Eidelman *et al.*, Eur. Phys. J. C **71**, 1534 (2011).
- [11] F. K. Guo, C. Hanhart, U. G. Meißner, Q. Wang and Q. Zhao, Phys. Lett. B **725**, 127 (2013).
- [12] B. Aubert *et al.* [BaBar Collaboration], Phys. Rev. Lett. **102**, 132001 (2009).
- [13] R. Aaij *et al.* [LHCb Collaboration], Nucl. Phys. B **886**, 665 (2014).
- [14] A. Denig, F. K. Guo, C. Hanhart and A. V. Nefediev, Phys. Lett. B **736**, 221 (2014).
- [15] J. H. Kühn, J. Kaplan and E. G. O. Safiani, Nucl. Phys. B **157**, 125 (1979).
- [16] K. A. Olive *et al.* (Particle Data Group), Chin. Phys. C **38**, 090001 (2014).
- [17] B. Aubert *et al.* [BaBar Collaboration], Phys. Rev. D **71**, 052001 (2005).
- [18] M. Ablikim *et al.* [BESIII Collaboration], Nucl. Instrum. Meth. A **614**, 345 (2010).
- [19] S. Agostinelli *et al.* [GEANT4 Collaboration], Nucl. Instrum. Meth. A **506**, 250 (2003).
- [20] J. Allison, *et al.*, IEEE Trans. Nucl. Sci. **53**, 270 (2006).
- [21] D. J. Lange, Nucl. Instrum. Meth. A **462**, 152 (2001).
- [22] R. G. Ping, Chin. Phys. C **32**, 599 (2008).
- [23] G. Bonneau and F. Martin, Nucl. Phys. B **27**, 381 (1971).
- [24] H. Czyż, A. Grzebińska and J. H. Kühn, Phys. Rev. D **81**, 094014 (2010).
- [25] V. P. Druzhinin, S. I. Eidelman, S. I. Serednyakov and E. P. Solodov, Rev. Mod. Phys. **83**, 1545 (2011).
- [26] M. Ablikim *et al.* [BESIII Collaboration], Phys. Rev. D **88**, 032007 (2013).
- [27] M. Ablikim *et al.* [BESIII Collaboration], arXiv:1503.03408 [hep-ex].
- [28] C. Z. Yuan [Belle Collaboration], arXiv:0910.3138 [hep-ex].
- [29] M. Ablikim *et al.* [BES Collaboration], Phys. Lett. B **659**, 74 (2008).